www.czasopisma.pan.pl PAN POLSKA AKADEMIA NAUK www.journals.pan.pl

A R C H I V E S O F M E T A L L U R G Y A N D M A T E R I A L S

Volume 60 2015 Issue 3

DOI: 10.1515/amm-2015-0387

W. DUDZIŃSKI*, Ł. KONAT*#, B. BIAŁOBRZESKA*

FRACTOGRAPHIC ANALYSIS OF SELECTED BORON STEELS SUBJECTED TO IMPACT TESTING

ANALIZA FRAKTOGRAFICZNA WYBRANYCH STALI Z BOREM W BADANIACH UDARNOŚCIOWYCH

In this paper dynamic properties of low-alloy boron steels – Hardox 500, B27 and HTK 900H in delivered state (after hardening and tempering) are considered. Charpy V-notch (CVN) test results in connection with fractography in the ductile-to-brittle transition temperature region were analyzed. Obtained from CVN test the impact transition curve, not always predicts properly a behavior of materials in conditions of dynamic loading. So an analyze of character of fracture helps to evaluate the real behavior of materials. Tested samples were cut out longitudinally in relation to cold work direction. The results of CVN test for selected steels, in temperatures: –40°C, –20°C, 0°C and +20°C are presented. Regarding ductile-to-brittle transition temperature, there is a significant difference taking into account values of Charpy V energy absorbed and a character of fracture.

Keywords: low alloy steels with boron, microstructural analysis, impact strength, fractography

W artykule przeprowadzono rozważania na temat dynamicznych właściwości niskostopowych stali z borem – Hardox 500, B27 oraz HTK 900H w stanie dostarczenia (po hartowaniu i odpuszczaniu). Przeprowadzono próbę udarności Charpy'ego w zakresie temperaturowego przejścia plastyczno-kruchego w powiązaniu z analizą fraktograficzną. Wyznaczona na podstawie wyników próby Charpy'ego udarnościowa krzywa przejścia, nie zawsze prawidłowo charakteryzuje zachowanie się materiału w warunkach obciążeń dynamicznych. Dlatego też fraktografia może uściślić rzeczywiste zachowanie się materiału. Próby przeprowadzono na próbkach wzdłużnych do kierunku przeróbki plastycznej w temperaturach: –40°C, –20°C, 0°C i +20°C. Stwierdzono występowanie znaczącej różnicy w określeniu temperatury przejścia w przypadku, gdy jest ona wyznaczona w oparciu o wynik próby udarności, a także gdy wyznaczono ją opierając się na charakterze przełomu.

1. Introduction

Today, under conditions of increasing demand in the industry for materials with very high strength, in the structural components appear varying impact loads characterized through a very sudden transition in the variation. This requires, in relation to the used structural materials, to identify individual properties and quality description expressed by the tendency of materials to transition in a brittle state due to the increased speed of the load. Therefore, in order to ensure safety during using, structural steel should maintain adequate strength not only static, but also should maintain the ability to elongation at a certain temperature. Impact test is an indicator of assessing the suitability of the steel just from the perspective of durability and protection against sudden destruction.

In recent years, high strength low-alloy boron steels, usually defined as high resistant to abrasive wear, become more widely used. To group of these steels are included, first and foremost, Hardox steels (ironworks SSAB) and other steel grades with similar properties. Boron steels include, for example [1,2]: Weldox, Domex i Armox (as well SSAB), Finnish steels Ovako i Ramor, Raex, B13, B24, B24CR, B27 and B27CR (Rautaruukki/SSAB), 20MCB5, 23MCB5, 28MCB5 and 30MCB5 (Zerneri Accai), XAR and TBL (ThyssenKrupp Steel Europe AG), Dillidur (Dillinger Hütte GTS), Durostat and Brinar (Grobblech GmbH), Fora and Creusabro (Industeel), Quard (NLMK Clabecq), HTK (Hut-Trans Katowice), Abrazo (TATA Steel Group), Endura (TITUS Steel), Sumihard (SUMITOMO Metal), JFE-EH (JFE EVERHARD Corporation), Armotec (Armotec Ltd). In many areas of the engineering industry these steels displace older materials, that may contribute to increasing the lifetime of components and give the possibility of a longer service life of the construction. A characteristic feature of these steels is their high

* WROCLAW UNIVERSITY OF TECHNOLOGY, DEPARTMENT OF MATERIALS SCIENCE, WELDING AND STRENGTH OF MATERIALS, 25 SMOLUCHOWSKIEGO STR., 50-370 WROCLAW, POLAND

Corresponding author: lukasz.konat@pwr.edu.pl

resistance to abrasive wear in combination with high mechanical properties, that are obtained through the homogeneity of the structure throughout the whole cross-section of the steel sheet. Homogeneity structure is obtained through a strictly-selected chemical composition, depended on the thickness of the steel sheet, that includes micro-addition of boron, low quantities of phosphorus and sulfur and through heat treatment or thermo-mechanical treatment. Producing process of steels with a high yield point and high strength may simultaneously lead to a significant reduction of ductility, especially at low temperatures.

Due to above considerations, mainly for the steel, there are many uncertainties in predicting the behavior of materials with the desired structure under dynamic loads. The criterion, that is most commonly used for limiting the possibility of use of any structural material, is a temperature of ductile-to-brittle transition. A common criterion for determining of brittleness threshold of structural steels is the adoption of some arbitrary value of the impact work or the impact strength. Often for structural steels it is amount equal to 35 J/cm^2 [3]. It is assumed that the criterion of impact strength corresponds to the occurrence of fracture in the mid-brittle and mid-ductile. However, this assumption is not always reliable, hence, the use of fractographic analysis allows to uniquely refer to the type and character of fracture.

The article studies focus on both, the analysis of the results of Charpy V-notch (CVN) test in connection with the analysis of obtained fracture. Moreover, the study is focused on a comparative analysis, in terms of impact properties and fractographic features of steel Hardox 500, HTK 900H and B27. The manufacturers produce Hardox 500 and HTK 700H steels that have undergone heat treatment, including quenching or quenching and tempering at low temperatures, while steel B27 is intended for heat treatment performing by their user. Structure in delivery state of B27 steel characterizes band distribution of ferrite and pearlite. After taking into account the purpose of the application of steel B27, this steel was heat-treated analogical to heat-treatment of steel Hardox 500 and HTK 900H, namely, quenched after austenitization at 930°C and as well tempered at 200°C.

2. Analysis of chemical composition

Chemical composition analysis was performed with a spectral method using glow discharge spectrometer GDS-750-QDP of LECO, using the following parameters: $U = 1250$ V, $I = 45$ mA, argon. The results were the average values of five measurements of chemical composition. Table 1 summarizes the results of the spectral analysis of the chemical composition of tested steels for sheet plates with a thickness of 8 and 10 mm.

Chemical composition analysis showed that the vast majority of the actual amounts of alloying elements are slightly lower than given by the manufacturers of the tested steel. Exceptions are slightly higher contents of chromium and silicon in steel B27. Generally, considered carbon content in the analyzed material is in the range 0.17-0.21%. The hardenability of tested steels was increased by introducing alloying elements such as chromium, nickel, manganese, molybdenum, and particularly boron. The presence of boron in the composition at an alloy value (0.0007÷0.001%) is a common feature of these steels. A content of nickel from 0.046 to about 0.11% is added to reduce the temperature of austenitizing and lower temperature of transition of the material to a brittle state. Carbide forming elements such as Cr, Mo, Ti, V, delay the start of diffusion processes, thus increasing the hardenability of the steel. In order to enhance this effect is often used molybdenum and chromium in combining. The presence of molybdenum in the steel composition is even more important that the chromium (and nickel and manganese with its presence) causes an increased in brittleness of the steel after tempering process. Aluminum and titanium were used as micro-alloying elements for the binding of nitrogen and to prevent of austenite grains growth during heat treatment. In addition, characteristic feature of analyzed steel is reduced content of harmful additives, such as sulfur (0.002÷0.005%) and phosphorus (0.007÷0.010%). Based on the contents of individual alloying elements, it can be concluded that analyzed steels belong to the group of low-alloy steel with boron [50-10].

TABLE 1

Chemical composition of steels Hardox 500 and HTK 900H (sheet plates with a thickness of 8 mm) and steel B27 sheet plates with a thickness of 10 mm) based on own analysis (W) and data given by the manufactures (P) [1,2,4,5]

Element [%wt.]	Hardox 500		B27		HTK 900H	
	– W –	– P –	– W –	– P –	– W –	– P –
C	0.170	0.270	0.212	0.270	0.120	0.180
Mn	0.995	1.600	0.730	1.200	0.410	1.500
Si	0.374	0.700	0.309	0.250	0.330	0.450
P	0.010	0.025	0.007	–	0.009	0.025
S	0.002	0.010	0.002	–	0.005	0.010
Cr	0.215	1.000	0.556	0.300	0.030	1.000
Ni	0.046	0.250	0.048	–	0.110	0.300
Mo	0.008	0.250	0.014	–	0.030	0.400
V	0.004	–	0.005	–	–	–
Cu	0.006	–	0.004	–	–	–
Al	0.035	–	0.057	–	–	–
Ti	0.020	–	0.003	0.040	–	–
Nb	0.010	–	0.005	–	–	–
Co	0.010	–	0.009	–	–	–
B	0.0016	0.0040	0.0007	0.002	0.001	–

3. Microstructural analysis

Light microscopy (LM) analysis of the microstructure was performed using a microscope NEOPHOT 32. It was used the magnification in range 25×÷2000×. Registration of the microstructures was performed with a digital camera Visitron Systems with software Spot Advanced. Observations at higher magnifications, and microanalysis of chemical composition, morphology, and nature of the phases were made using a scanning electron microscope (SEM), JSM-5800LV Jeol coupled with X-ray micro-analyzer Oxford Link ISIS-300. Accelerating

voltage used during the research was 20 and 25 kV. Observations of the microstructures were carried out in material contrast using SE and BSE detectors. Before microscopic observations the specimens were sputtered with the amorphous carbon. The results of microscopic analysis are shown at Figs. 1÷3.

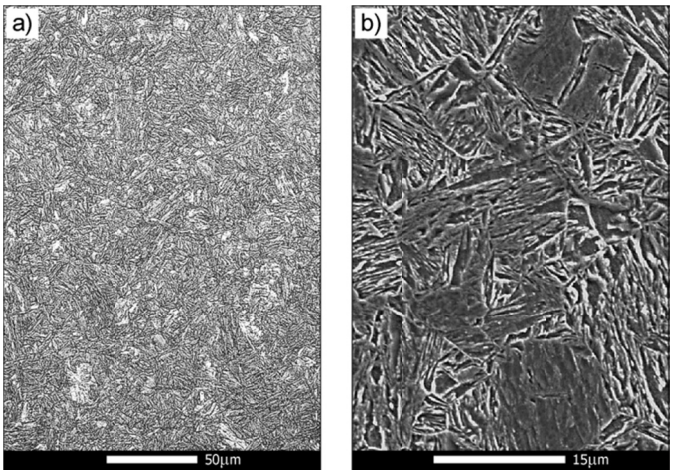

Fig. 1. Microstructure of steel Hardox 500 in delivery condition [1]: a) LM; b) SEM. Etched with 3%HNO_3

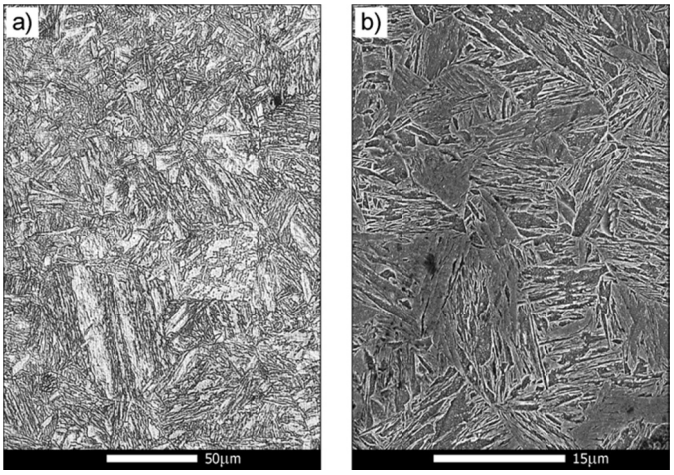

Fig. 2. Microstructure of steel B27 after hardening and tempering at 200°C [2]: a) LM; b) SEM. Etched with 3%HNO_3

In the delivery state, steel Hardox 500 is characterized by a homogeneous structure of tempering martensite with large number of precipitates of carbide phases distributed primarily within the martensite laths (Fig. 1). In addition, the areas in which the former austenite grain boundaries are reflected can be distinguished. During the study with using the methods of transmission electron microscopy (TEM) and diffractograms analysis of tested steel it was showed the presence of large number of carbide phases distributed in large agglomerations [1]: MoC, Mo_2C, MoCrC, Cr_3C, Cr_3C_2, Cr_7C_3, $Cr_{23}C_6$, Ti_2C, Nb_3C_2.

Steel B27 after hardening and tempering at 200°C shows the martensitic structure (tempering martensite) with precipitates of fine carbides within the martensite laths (Fig. 2b). The former austenite grain boundaries are clearly marked (Fig. 2a). During the study with using the methods of transmission electron microscopy (TEM) and diffractograms analysis of tested steel it was showed the presence of large number of carbide phases type [2] MoC, Cr_7C_3, $Cr_{23}C_6$, Cr_3C_2 and borides type $M_{23}B_6$. Carbide phases were located mainly inside, but only sometimes on the borders of martensite laths. In areas with carbide phases there were also observed significantly higher density of dislocations.

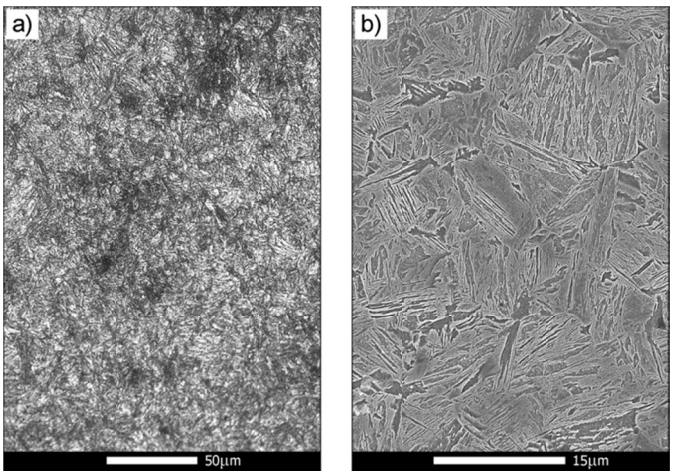

Fig. 3. Microstructure of steel HTK 900H in delivery condition [4]: a) LM; b) SEM. Etched with 3%HNO_3

In the delivery state, steel HTK 900H is also characterized by a structure of tempering martensite with low number of precipitates of carbide phases (Fig. 3b). Moreover, some areas with a bainitic structure and ferrite grains were found (Fig. 3a). In the case of steel HTK 900H the study using transmission electron microscopy TEM were not performed.

4. Impact strength results

Impact strength tests were carried out using the Charpy impact test (KV150) according to standard PN-EN 10045-1. Samples were taken longitudinally to the direction of plastic forming of materials. In order to determine the curve of ductile-to-brittle transition, the impact work was determined for the following temperatures: –40°C, –20°C, 0°C and + 20°C. The strength results are shown graphically in Fig. 4.

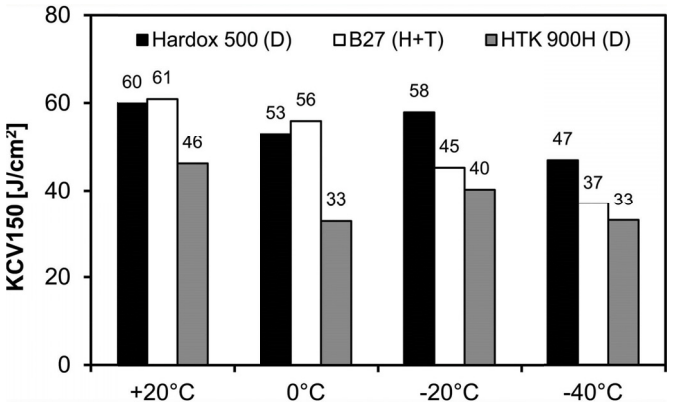

Fig. 4. Changes in impact strength of tested steel in a function of temperature [1,2,4]: (D) – delivery state, (H+T) – state after hardening and tempering

The tested materials are characterized through different resistance to brittle fracture, that in many application has fundamental meaning. Comparing the obtained values of impact work of the examined steels, it can be considered that the steel HTK 900H was characterized through a lowest value of impact strength at each temperature of the test. The impact strength of this steel in delivery condition at a temperature range of test from –40°C to +20°C was 33÷46 J/cm^2, however, any sharp decline in the toughness of the steel wasn't noted. Taking the criterion of minimum impact strength equal to 35 J/cm^2, this steel meets this criterion in delivery state at temperatures of 20°C and –20°C. However, at temperatures of 0°C and –40°C, the impact strength of this steel was 33 J/cm^2 and was not much lower than the taken criterion. Steel B27 after hardening and tempering and steel Hardox 500 in delivery condition are characterized by similar values of impact strength. In contrast to steel HTK 900H, the values of impact strength of these steels meet the criterion cited throughout the whole range of test temperatures.

5. Fractographic analysis

Figs. 5 and 6 summarize the macroscopic view of fractures of tested steels at temperatures of +20°C and –40°C for delivery state and after heat treatment. Figs. 7÷12 show representative images of fracture surfaces of investigated steels obtained using scanning electron microscope.

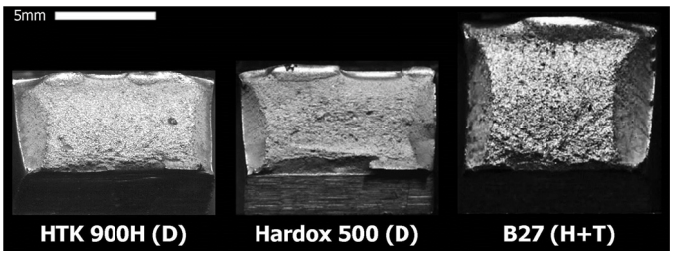

Fig. 5. Macroscopic view of fracture of investigated steels [1,2,11]. Test temperature: +20°C, (D) – delivery state, (H+T) – hardened and tempered state

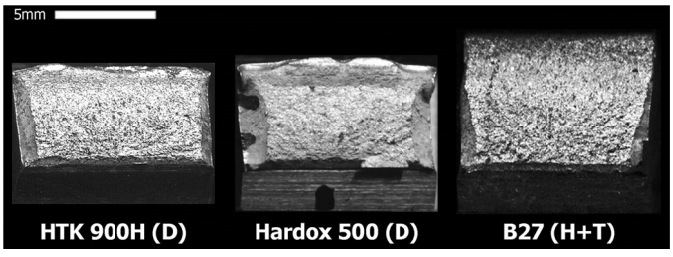

Fig. 6. Macroscopic view of fracture of investigated steels [1,2,11]. Test temperature: –40°C, (D) – delivery state, (H+T) – hardened and tempered state

5.1. Steel Hardox 500 – fracture at temperatures of +20°C and –40°C

Fractures of test samples of steel Hardox 500, after test at temperature of +20°C have ductile character (Fig. 7). Their structure has characteristic morphology of cavities with different diameter, ie. about 25 and 5 μm. Most frequently in cavities with a larger diameter is noticed the presence of the precipitates of carbide phases. In case of investigated steel significantly larger area is occupied by cavities about the size of 5 μm. In some grains there can be visible some areas of cleavage fracture. This type of fracture of the steel reduces its toughness and impact strength, but nevertheless allows to achieve a relatively high its level of 60 J/cm^2. Fracture of samples of steel Hardox 500, after the impact test at temperature of –40°C has cleavage character (Fig. 8). However, there can be distinguish several areas of ductile fracture. This type of fractures in case of steel Hardox 500 allows to achieve relatively high value of impact strength amounting to 47 J/cm^2 [1,12].

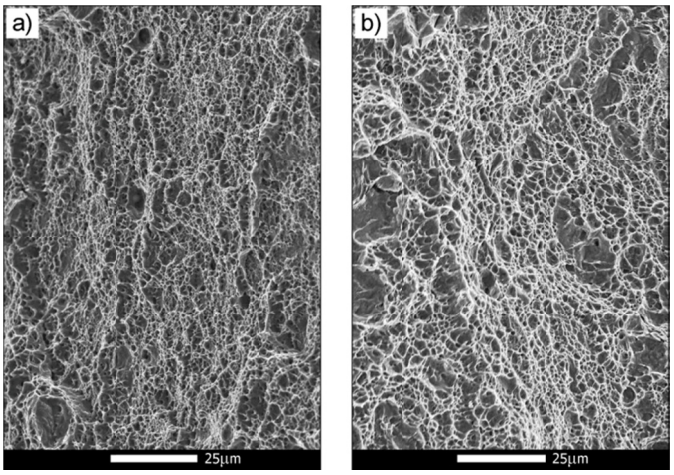

Fig. 7. Microscopic view of fracture of steel Hardox 500 in delivery state [1,12]: a) zone under mechanical notch; b) central zone. Test temperature: +20°C, non-etched state, SEM

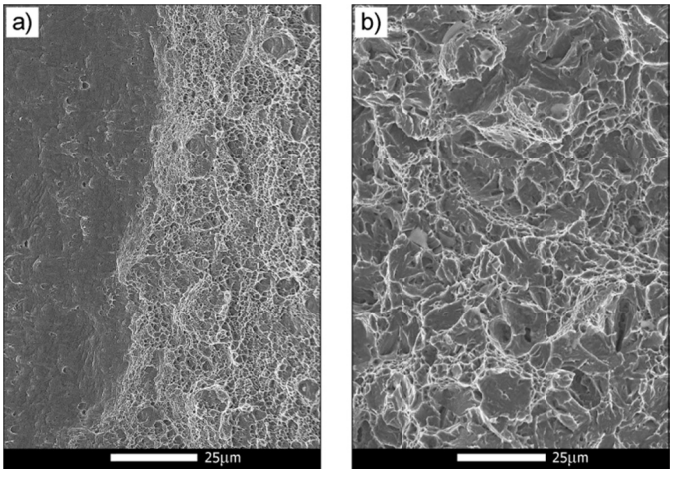

Fig. 8. Microscopic view of fracture of steel Hardox 500 in delivery state [1,12]: a) zone under mechanical notch; b) central zone. Test temperature: –40°C, non-etched state, SEM

5.2. Steel B27 – fracture at temperatures of +20°C and –40°C

The view of fracture of steel B27 under mechanical notch at temperature of +20°C was shown at Fig. 9a. Characteristic for this fracture is cavity surface with various size of the holes, as a results of various size, relatively rarely distributed intermetallic precipitates. The middle zone of fracture of the steel B27 presents ductile character with small areas of facets (Fig. 9b). The areas of the small facets are connected through plastic deformation, and between them there are formed plastic substructures, which indicates to a large plastic deformation during the formation of the fracture.

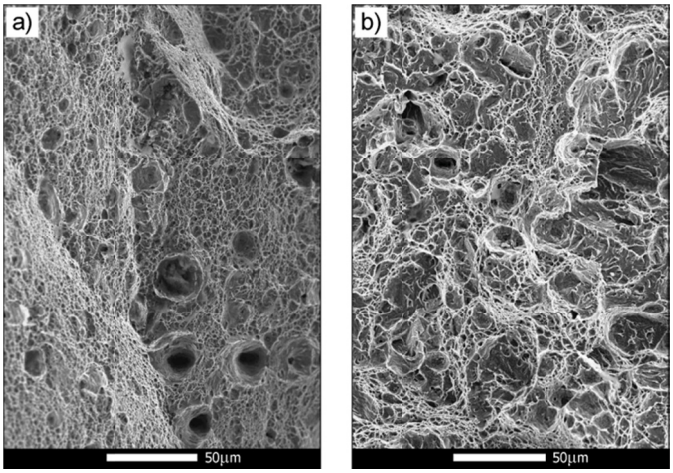

Fig. 9. Microscopic view of fracture of steel B27 after hardening and tempering [2]: a) zone under mechanical notch; b) central zone. Test temperature: +20°C, non-etched state, SEM

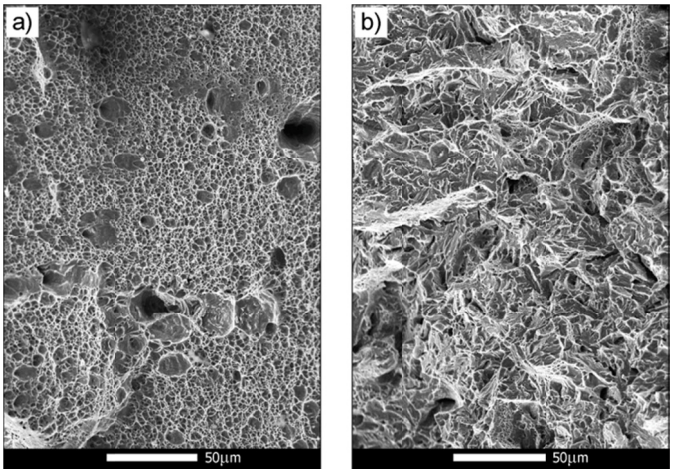

Fig. 10. Microscopic view of fracture of steel B27 after hardening and tempering [2]: a) zone under mechanical notch; b) central zone. Test temperature: -40°C, non-etched state, SEM

Impact strength of steel B27 at lowest temperature of the test is higher than the value of 35 J/cm^2 at which the transition ductile – to – brittle takes place, however, the character of fracture changed slightly. Relatively large plastic lateral areas and as well zones under mechanical notch (Fig. 10a) represent ductile fracture with cavities with different diameters. The central zone is a fracture defined as quasi-cleavage (Fig. 10b). This kind of fracture is formed by cleavage cracks in small local areas and their connection in one cracking surface due to plastic deformation. Although these facets are similar to cleavage facets due to the presence of river pattern, the identification of crystallographic planes is almost impossible. Bridges of quasi-cleavage facets have developed topography, which also indicates to a large plastic deformation during their creation. Thus received facets are small, with no clear boundaries. This kind of fracture providing a significant reserve of ductility of the steel and can be considered as not exceeding the brittleness threshold till the temperature of –40°C. Characteristic feature of quasi-cleavage is furthermore transition of faults of secondary cleavage into bridges surrounding the facets. Characteristic features of ductile fracture as cavities can be also noticed [2].

5.3. Steel HTK 900H – fracture at temperatures of +20°C i –40°C

Near to mechanical notch of the steel HTK 900H occurs ductile fracture with characteristic cavity structure (Fig. 11a). In large but relatively shallow holes are visible brittle precipitations of intermetallic phases, which were initiators of the crack. Towards into central zone ductile fracture becomes to the mostly brittle fracture. Central zone has developed topography, with many faults (Fig. 11b). In addition, it can be noticed characteristic rivers patterns characteristic for a brittle fracture.

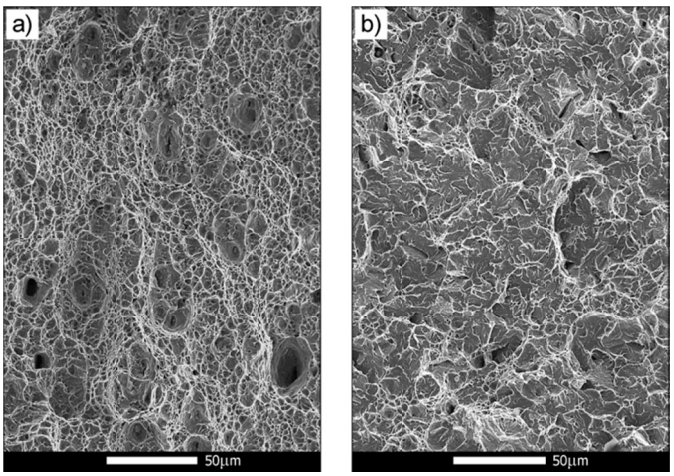

Fig. 11. Microscopic view of fracture of steel HTK 900H in delivery state [4], [11]: a) zone under mechanical notch; b) central zone. Test temperature: +20°C, non-etched state, SEM

In temperature of –40°C character of fracture does not change significantly. Near to mechanical notch of steel occurs ductile fracture with small, vestigial areas of brittle fracture (Fig. 12a). Middle zone of fracture of investigated steel is a quasi-cleavage fracture with developed topography (Fig. 12b).

Areas between the facets have a features of ductile fracture, what indicates to large plastic deformation during their formation. This increase in the share of plastic deformation is reflected by the formation of shallow deformed holes between the facets. Participation of ductile fracture in the central zone comprises not more than 5 to 10% of the fracture surface.

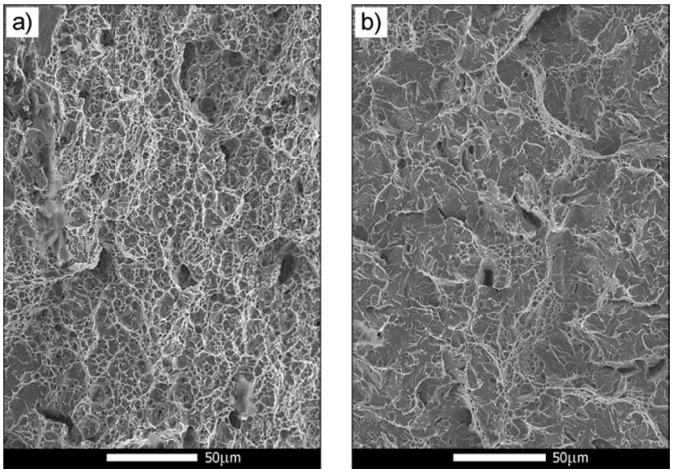

Fig. 12. Microscopic view of fracture of steel HTK 900H in delivery state [4], [11]: a) zone under mechanical notch; b) central zone. Test temperature: –40°C, non-etched state, SEM

6. Conclusions

In the study, three different low-alloy boron steels with high resistance to abrasion wear were the subject of comparison analysis. During carried out chemical analyzes it was demonstrated that strictly selected chemical composition of these steels allows to obtain high strength while maintaining relatively high levels of elongation and impact strength. Obtaining a beneficial indicators of impact work results directly from the similar microstructure of investigated steels. Research using light and electron microscopy methods showed the presence in them coherent carbide phases mainly distributed within the martensite laths. Such a distribution of precipitates blocks a dislocation movement, causing strengthening of the steel. Coherent composition of carbide phases in the investigated steels also excludes the possibility of chipping them from the metallic matrix.

Fractographic analysis showed that all analyzed steels are characterized by significant participation of ductile fracture. After impact test at temperature of +20°C there are visible large plastic lateral areas and fine-grained central zone. Relatively large lateral areas with plastic features and clearly marked zone of ductile fracture under mechanical notch are retained even at the lowest test temperature, especially in case of steel Hardox 500. At temperature of –40°C fracture of steel Hardox 500, in central zone, is characterized also through randomly distributed fragment of ductile and cleavage fracture. Fragments of cleavage fracture are characterized through fine facets with occurring slip. Steels B27 after hardening and tempering and Hardox 500 in delivery condition achieve similar value of impact strength. For these steels values of impact strength remain above the taken criterion of minimum impact strength equal to 35 J/cm^2, which is adapted for structural materials in many applications, in whole temperature range of the test.

REFERENCES

[1] Ł. Konat, Struktury i właściwości stali Hardox a ich możliwości aplikacyjne w warunkach zużywania ściernego i obciążeń dynamicznych, Rozprawa doktorska, Politechnika Wrocławska, Wydział Mechaniczny, Instytut Materiałoznawstwa i Mechaniki Technicznej, Seria PRE, 3, 2007.

[2] B. Łętkowska, Wpływ obróbki cieplnej na strukturę i wybrane własności stali gatunku B27 oraz 28MCB5, Rozprawa doktorska, Politechnika Wrocławska, Wydział Mechaniczny, Instytut Materiałoznawstwa i Mechaniki Technicznej, Seria PRE, 2, 2013.

[3] J.W. Wyrzykowski, E. Pleszakow, J. Sieniawski, Odkształcenie i pękanie metali, WNT, Warszawa 1999.

[4] B. Łętkowska, Badania materiałowe stali HTK-700H i HTK-900H, a możliwości ich zastosowania w konstrukcji maszyn górnictwa odkrywkowego, praca dyplomowa – magisterska, Politechnika Wrocławska, Wydział Mechaniczny, Instytut Materiałoznawstwa i Mechaniki Technicznej, 2007

[5] Hardox – Das Verschleiβblech der vielen Möglichkeiten, Wyd. SSAB Oxelösund, 2002.

[6] M. Blicharski, Inżynieria Materiałowa – Stal, WNT, Warszawa 2004.

[7] T. Malkiewicz, Metaloznawstwo stopów żelaza, PWN, Warszawa-Kraków 1968.

[8] J. Kowalski, J. Pstruś, S. Pawlak, M. Kostrzewa, R. Martynowski, W. Wołczyński, Influence of the Reforging Degree on the Annihilation of the Segregation Defects in the Massive Forging Ingots, Archives of Metallurgy and Materials **56**, 1029-1043 (2011) .

[9] W. Wołczyński, E. Guzik, W. Wajda, D. Jędrzejczyk, B. Kania, M. Kostrzewa, CET in Solidifying Roll – Thermal Gradient Field Analysis, Archives of Metallurgy and Materials **57**, 105-117 (2012).

[10] T. Himemiya, W. Wołczyński, Prediction of Solidification Path and Solute Redistribution of an Iron-based Multi-Component Alloy Considering Solute Diffusion in the Solid, Materials Transactions of the Japan Institute of Metals **43**, 2890-2896 (2002).

[11] S. Frydman, Ł. Konat, B. Łętkowska, G. Pękalski, Impact resistance and fractography of low-alloy martensitic steels, Archives of Foundry Engineering **8**, spec. iss. 1, 89-94 (2008).

[12] S. Frydman, Ł. Konat, G. Pękalski, Analiza fraktograficzna stali Hardox 400 i Hardox 500 w badaniach udarnościowych, Górnictwo Odkrywkowe, R. 49, 3/4, 36-47 (2007).

Received: 20 April 2015